

Impaired Conduction in the Bundle Branches of Mouse Hearts Lacking the Gap Junction Protein Connexin40

Harold V.M. van Rijen, PhD; Toon A.B. van Veen, MSc; Marjan J.A. van Kempen, PhD; Francien J.G. Wilms-Schopman, RT; Mark Potse, MSc; Olaf Krueger, MSc; Klaus Willecke, PhD; Tobias Opthof, PhD; Habo J. Jongsma, PhD; Jacques M.T. de Bakker, PhD

Background—Connexin (Cx)40 and Cx45 are the major protein subunits of gap junction channels in the conduction system of mammals. To determine the role of Cx40, we correlated cardiac activation with Connexin distribution in normal and Cx40-deficient mice hearts.

Methods and Results—Epicardial and septal activation was recorded in Langendorff-perfused adult mice hearts with a 247-point compound electrode (interelectrode distance, 0.3 mm). After electrophysiological measurements, hearts were prepared for immunohistochemistry and histology to determine Connexin distribution and fibrosis. In both wild-type and Cx40-deficient animals, epicardial activation patterns were similar. The right and left ventricular septum was invariably activated from base to apex. Histology revealed a continuity of myocytes from the common bundle to the septal myocardium. Within this continuity, colocalization was found of Cx43 and Cx45 but not of Cx40 and Cx43. Both animals showed similar His-bundle activation. In Cx40-deficient mice, the proximal bundle branches expressed Cx45 only. The absence of Cx40 in the proximal bundles correlated with right bundle-branch block. Conduction in the left bundle branch was impaired as compared with wild-type animals.

Conclusions—Our data show that (1) in mice, a continuity exists between the common bundle and the septum, and (2) Cx40 deficiency results in right bundle-branch block and impaired left bundle-branch conduction. (*Circulation*. 2001; 103:1591-1598.)

Key Words: proteins ■ bundle-branch block ■ conduction ■ immunohistochemistry ■ mapping

Electrical coupling of myocytes by gap junctions permits intercellular current flow, a prerequisite for cardiac conduction. Gap junctions are agglomerates of individual channels that directly connect the cytoplasm of adjacent cells. Gap junction channels are formed by head-to-head alignment of 2 hexameric hemichannels, each composed of 6 Connexin (Cx) molecules. At least 4 different cardiac connexins have been reported. Cx37 is found in rabbit endocardium,¹ Cx40 is mainly found in the atrium and conduction system,²⁻⁸ and Cx43 is located in the atrial and ventricular myocardium and in the distal parts of the conduction system.^{4,5,8} Finally, Cx45 is present throughout the heart in small amounts,^{6,7,9,10} with some overexpression in the conduction system.^{11,12}

Mice lacking the gene for Cx40 exhibit reduced atrial but not ventricular conduction velocity.¹³ The ECGs of Cx40 knockout mice have prolonged P waves, in agreement with reduced atrial conduction velocity. Moreover, the PR interval is prolonged, suggestive for atrioventricular (AV) nodal dysfunction.¹⁴⁻¹⁶ Also, QRS complexes of these animals are

prolonged.¹⁴⁻¹⁶ Impaired function of the specific conduction system probably explains the prolonged QRS duration because Cx40 is normally not expressed in working ventricular myocardium.

The purpose of this study was to determine the role of Cx40 in propagation of the electrical impulse in the specific conduction system of the mouse heart.

Methods

Animals

All mice of mixed genetic background (Cx57BL/6 and 129Sv) were generated and bred at the Institute of Genetics, University of Bonn (Germany), and genotyped by polymerase chain reaction as described.¹⁵ In total, 12 wild-type and 12 Cx40^{-/-} littermates between 4 and 6 months of age were used for experiments. The study conformed to the guiding principles of the American Physiological Society.

Preparation of Hearts

Mice were anesthetized by intraperitoneal injection of urethane (2 g/kg body wt). The chest was opened and the heart was excised and

Received July 14, 2000; revision received September 15, 2000; accepted September 21, 2000.

From the Department of Medical Physiology (H.V.M.v.R., T.A.B.v.V., M.J.A.v.K., T.O., H.J.J.), Utrecht, The Netherlands; Interuniversity Cardiology Institute of the Netherlands (F.J.G.W.-S., J.M.T.d.B.), Utrecht, The Netherlands; the Department of Medical Physics (M.P.), Academic Medical Center, Amsterdam, The Netherlands; the Institute of Genetics (O.K., K.W.), University of Bonn, Germany; and the Department of Cardiology (J.M.T.d.B.), University Medical Center, Utrecht, The Netherlands.

Correspondence to Harold V.M. van Rijen, PhD, Department of Medical Physiology, Faculty of Medicine, University of Utrecht, PO Box 80043, 3508 TA Utrecht, The Netherlands. E-mail H.V.M.vanRijen@med.uu.nl.

© 2001 American Heart Association, Inc.

Circulation is available at <http://www.circulationaha.org>

submerged in Tyrode's solution¹⁷ at 4°C. With the aid of a binocular microscope, the heart was dissected from the lung as well as other tissue and the aorta was cannulated. Subsequently, the heart was connected to a Langendorff perfusion setup and perfused at 37°C and perfusion pressure of 80 cm H₂O. Perfusion buffer composition was (in mmol/L): NaCl 90, KCl 3.6, KH₂PO₄ 0.92, MgSO₄ 0.92, NaHCO₃ 19.2, CaCl₂ 1.8, glucose 22, creatine 6, taurine 6, and insulin 0.1 μmol/L, gassed with 95% O₂ and 5% CO₂. In all experiments, the heart started to beat immediately after initiating perfusion. Flow rate was ≈2 mL/min. To ensure proper temperature of the preparation, the heart was placed against a heated (37°C) and continuously moisturized support.

Recording of Electrograms

Extracellular electrograms were recorded with a 247-point multiterminal electrode, mounted in a micromanipulator. Electrodes were silver wires with a diameter of 0.1 mm that were isolated except at the tip. Electrode terminals were arranged in a 19×13 grid at interelectrode distances of 0.3 mm. Recordings were made in unipolar mode with regard to a reference electrode connected to the support of the heart. Electrograms were acquired with the use of a custom-built, 256-channel, data-acquisition system. Signals were bandpass-filtered (low cut-off, 0.16 Hz [12 dB]; high cut-off, 1 kHz [6 dB]) and digitized with 16-bit resolution at a bit step of 2 μV and a sampling frequency of 2 kHz. The input noise of the system was 4 μV (peak-peak). Data were acquired at a sample rate of 2 kHz.

Epicardial recordings of the ventricles were made in sinus rhythm and paced rhythm [wild-type (knockout): left ventricle, n=12 (11); right ventricle n=12 (11)]. For the latter, a bipolar silver wire (diameter of poles, 0.1 mm; interelectrode distance, 0.2 mm) was positioned on one of the atria. Pacing was performed with a Grass bipolar isolated stimulator. Stimulus trains were generated by a Macintosh computer equipped with an AD board and custom-written software.

For septal measurements, the right and left ventricular free walls were removed. Surgical resection of the free wall sometimes resulted in AV block, thus prohibiting the recording of bundle activation. The electrode grid was positioned in basal position on the interventricular septum. Reliable determination of conduction velocity required electrograms at 4 adjacent electrodes [wild-type (knockout): left bundle branch (LBB), n=4 (3); right bundle branch (RBB), n=6 (12)]. AV nodal conduction curves were determined [wild-type (knockout): n=5 (5)]. The atrium was stimulated at a cycle length of 100 ms. Every 16th stimulus was followed by 1 premature stimulus. Starting at 90 ms, the coupling interval of the extra stimulus was reduced in steps of 5 ms until AV block occurred. We used the time constant of the conduction curve fitted to a monoexponential function as a measure for progressively increasing AH delay. His bundle measurements were made after opening of the right atrium. Subsequently, the center of the electrode grid was positioned on the coronary sinus and recordings were made [wild-type (knockout): n=3 (2)].

Data Analysis

Activation maps were constructed from the activation times, determined with custom-written software based on Matlab (The Mathworks Inc). The moment of maximal negative dV/dt in the unipolar electrograms was selected as the time of local activation.

Activation times of the ventricular epicardia were corrected for sinus rhythm frequency by the use of the conduction curves of the His bundle.

Statistics

All numerical values are given as mean±SEM. Statistical comparisons were performed with an unpaired Student's *t* test, with StatView 4.5. A probability value of 0.05 was regarded as statistically significant.

Immunohistochemistry and Histology

Connexin expression was compared between Cx40-deficient (n=5) and wild-type littermates (n=5). The hearts were connected to the

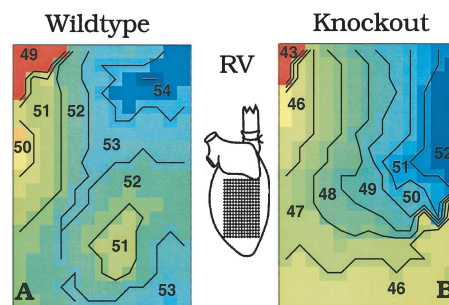


Figure 1. Epicardial activation patterns of right ventricle (RV) of wild-type (A) and Cx40-deficient (B) mouse hearts in sinus rhythm. Activation times are calculated with respect to first atrial activation. In wild-type, earliest epicardial activation (red sites) was found at basal site (A). In Cx40-deficient heart, earliest activation was also found at basal site (B).

Langendorff setup for several minutes to remove blood. The hearts were rapidly frozen in liquid nitrogen and stored at -80°C.

The hearts were serially sectioned in frontal plane with a cryostat to produce 4-chamber-view sections. Sections incorporating the conduction system were incubated with primary antibodies directed against Cx40, Cx43, and Cx45. Desmin was used as a marker for the conduction system. Primary antibodies were visualized with fluorescent secondary antibodies as described previously.¹⁸ Sections were stained with picrosirius red and examined by light microscopy for assessment of fibrosis.¹⁹

Results

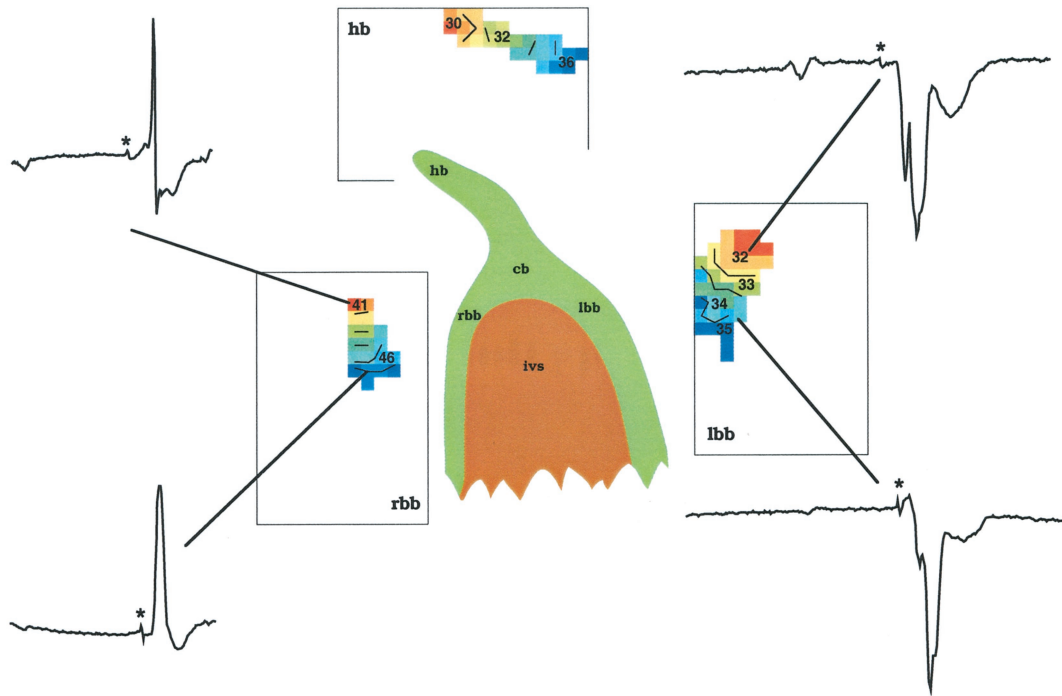
Wild-type and Cx40-deficient mouse hearts did not differ in morphology or heart weight. In wild-type mice, gap junctions between atrial myocytes were composed of Cx40 and Cx43, whereas only Cx43 was detected in ventricular myocytes. In Cx40-deficient animals, only Cx43 was found in atrial myocardium.

Epicardial Connexin Expression and Activation Patterns

Epicardial activation patterns were determined during sinus rhythm (R-R interval, 172±6.8 and 188±13.8 ms in wild-type and knockout hearts, respectively) and were not significantly different between wild-type and knockout mice (*P*=0.3). In 10 of 12 wild-type hearts, earliest epicardial activation of the right ventricle was found at the basal site, of which 8 had a second early activated area at the apex or the septal/lateral wall (Figure 1A). In the other 2 hearts, breakthrough activation was found in the mid free wall. Similarly, 10 of 11 Cx40-deficient hearts showed earliest activation at the basal site, 8 of which also had second early sites at the apex of the septal/lateral wall (Figure 1B). In the remaining hearts, apical activation was found. Left epicardial activation was similar to right ventricular activation of both wild-type and knockout mice, also showing predominant basal earliest activation.

In wild-type animals, average corrected right ventricular activation occurred 4.8 ms earlier than left ventricular activation, whereas in knockout animals the opposite was found. Right ventricular activation was 2.6 ms later than left ventricular activation (*P*=0.01).

Wildtype



Knockout

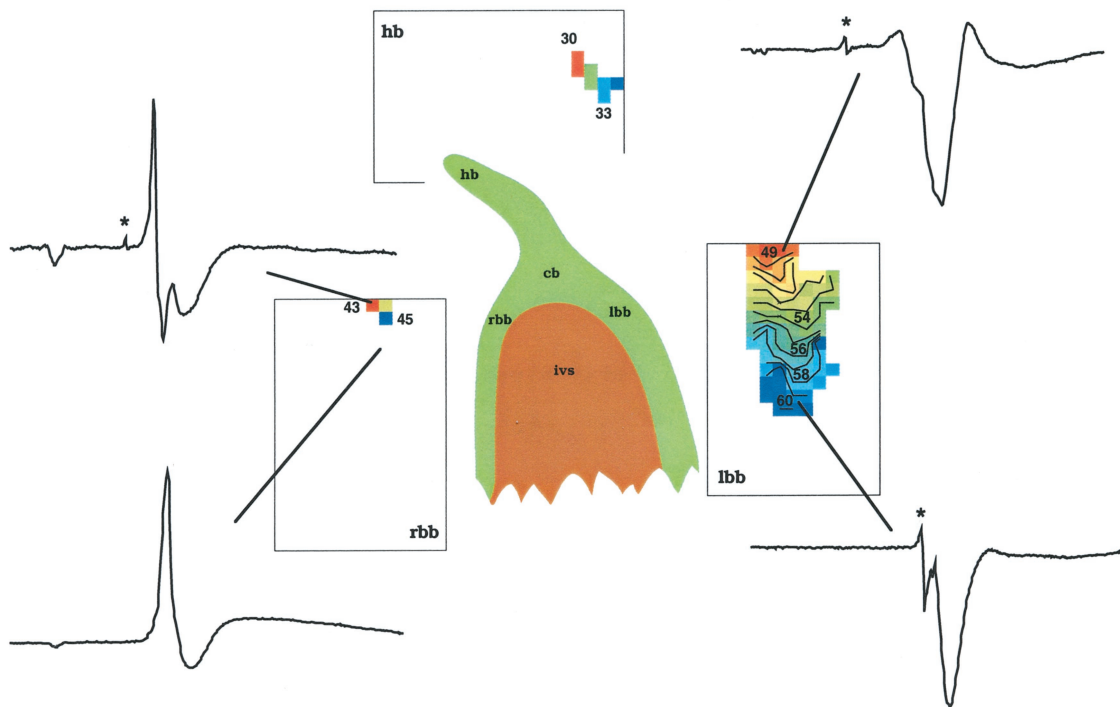


Figure 2. Typical examples of bundle-branch activation on both left and right septum in wild-type (upper panels) and Cx40 knockout animals (lower panels). After removal of ventricular free walls, electrode grid was positioned on septum while the heart was paced on atrium by separate stimulus electrode. Top panels show activation of His bundle (hb). Electrograms of representative individual electrodes show remote P wave ($t=0$ at onset of P wave) followed by bundle-branch signal (marked by asterisk). Large complex reflects activation of interventricular septum (ivs). Note premature block of right bundle branch (rbb) in Cx40 knockout animals. Left bundle branch (lbb) activation is significantly slower in knockout animals, whereas His-bundle activation is not altered. cb indicates common bundle.

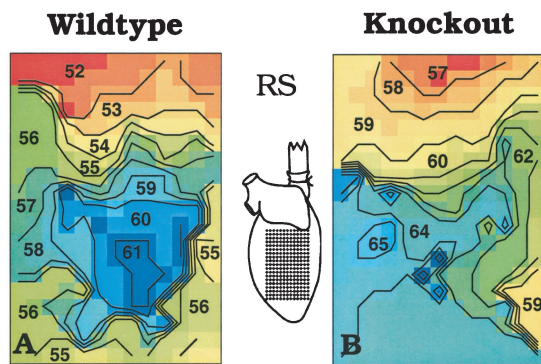


Figure 3. Activation patterns of right interventricular septum (RS) in wild-type (A) and Cx40 knockout animals (B). Septal activation is always observed from base (top) to apex (bottom).

Bundle-Branch Conduction and Septal Activation

After removal of the left and right ventricular free walls, the electrode grid was positioned against the left or right septal wall. The stimulation electrode was placed on one of the atria to pace the heart at a constant rate. Figure 2 shows typical examples of activation patterns of the conduction system. LBB deflections (marked by asterisk in right panels) were found in all experiments on both wild-type and Cx40-deficient animals. RBB signals (asterisk in left panels) were recorded in all wild-type animals. However, in only 1 of 12 Cx40-deficient hearts, full RBB activation was measured. In 3 (of 12) Cx40-deficient hearts, RBB activation blocked at 0.3 or 0.6 mm from the AV groove (as shown in Figure 2), whereas in the other 8 hearts, no RBB signals could be detected.

In wild-type hearts, conduction velocities in the LBB and RBB were $0.42 \pm 0.03 \text{ m} \cdot \text{s}^{-1}$ and $0.31 \pm 0.04 \text{ m} \cdot \text{s}^{-1}$, respectively. Conduction velocity in the His bundle ($0.52 \pm 0.15 \text{ m} \cdot \text{s}^{-1}$) was always faster than in the bundle branches.

In Cx40 knockout mice (Figure 2), the conduction velocity in the LBB was $0.28 \pm 0.02 \text{ m} \cdot \text{s}^{-1}$, significantly lower as compared with wild-type mice ($P=0.01$). RBB activation conducted at $0.32 \text{ m} \cdot \text{s}^{-1}$. In Cx40 knockout hearts, conduction velocity in the His bundle was high (0.64 ± 0.37) and not significantly different from wild-type hearts ($P=0.76$).

Figure 3 shows typical examples of right septal activation patterns in wild-type (Figure 3A) and Cx40-deficient hearts (Figure 3B). In both the wild-type and Cx40-deficient mice, earliest septal activation was seen invariably at the base. Activation patterns of the left interventricular septum were identical to the right septum.

AV Conduction Characteristics

Figure 4 shows a typical example of a conduction curve. The AH delay increases exponentially with decreasing coupling interval, being almost identical in wild-type and Cx40-deficient animals. The time constants of the conduction curves in both wild-type and Cx40-deficient animals were similar and not statistically different (wild-type, $20.8 \pm 3.9 \text{ ms}$; Cx40 knockout, $20.7 \pm 4.5 \text{ ms}$; $P=0.99$). Also, the maximal increase in delay was not different as well (wild-type, $21.5 \pm 3.7 \text{ ms}$; Cx40 knockout, $23.6 \pm 2.7 \text{ ms}$; $P=0.68$).

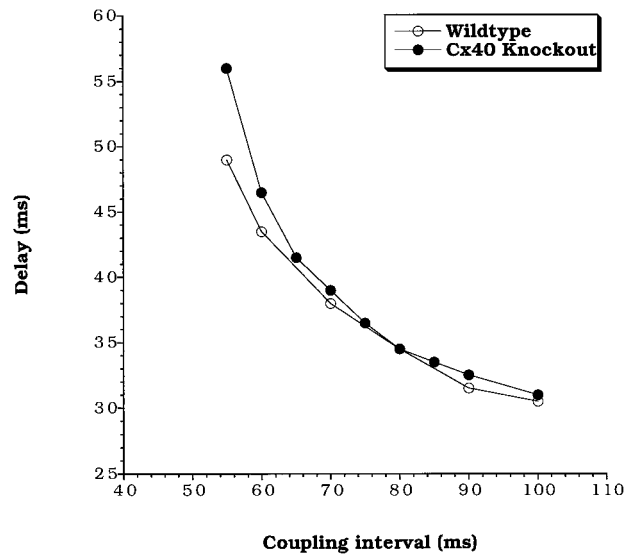


Figure 4. Typical example of A-H delay of wild-type (○) and Cx40 knockout (●) mice. No statistically significant differences were found between knockout and wild-type animals.

Even though activation in the RBB blocks after 0.3 to 0.6 mm below the AV groove in Cx40-deficient animals, the activation times recorded at these proximal electrodes are not different from control.

Connexin Distribution in and Histology of the Septum and Common Bundle

Figure 5 shows sections of the septum containing the conduction system of both wild-type and Cx40-deficient hearts, illustrating the distribution of Cx40, Cx43, Cx45, and desmin.

Cx40 Expression

In wild-type mice, Cx40 is abundantly expressed in the His bundle, common bundle, and bundle branches (Figure 5A). The Cx40 distribution indicates that the LBB is much wider than the RBB. Cx40 was absent in the bundle branches of Cx40-deficient mice (Figure 5B).

Cx43 Expression

In both wild-type and Cx40-deficient hearts, Cx43 was expressed in the septal region of the heart but not in the proximal conduction system (Figure 5, C and D).

Cx45 Expression

In both wild-type and Cx40-deficient hearts, Cx45 staining was found in the His bundle, the common bundle, proximal bundle branches, and Purkinje system but not in the septal regions (Figure 5, E and F).

Coexpression of Cx40, Cx43, and Cx45

Figure 6A shows a double labeling of Cx40 (green) and Cx43 (red). Cx40 was found in the common bundle and bundle branches (marked by desmin in consecutive section in Figure 6C) and Cx43 in the septum. No colocalization of Cx43 and Cx40 was found. Figure 6B shows that the expression of Cx45 (green) extended from the common bundle toward the septum, where Cx43 (red) is expressed. Cx43 and Cx45 colocalize in the cells between the common bundle and the

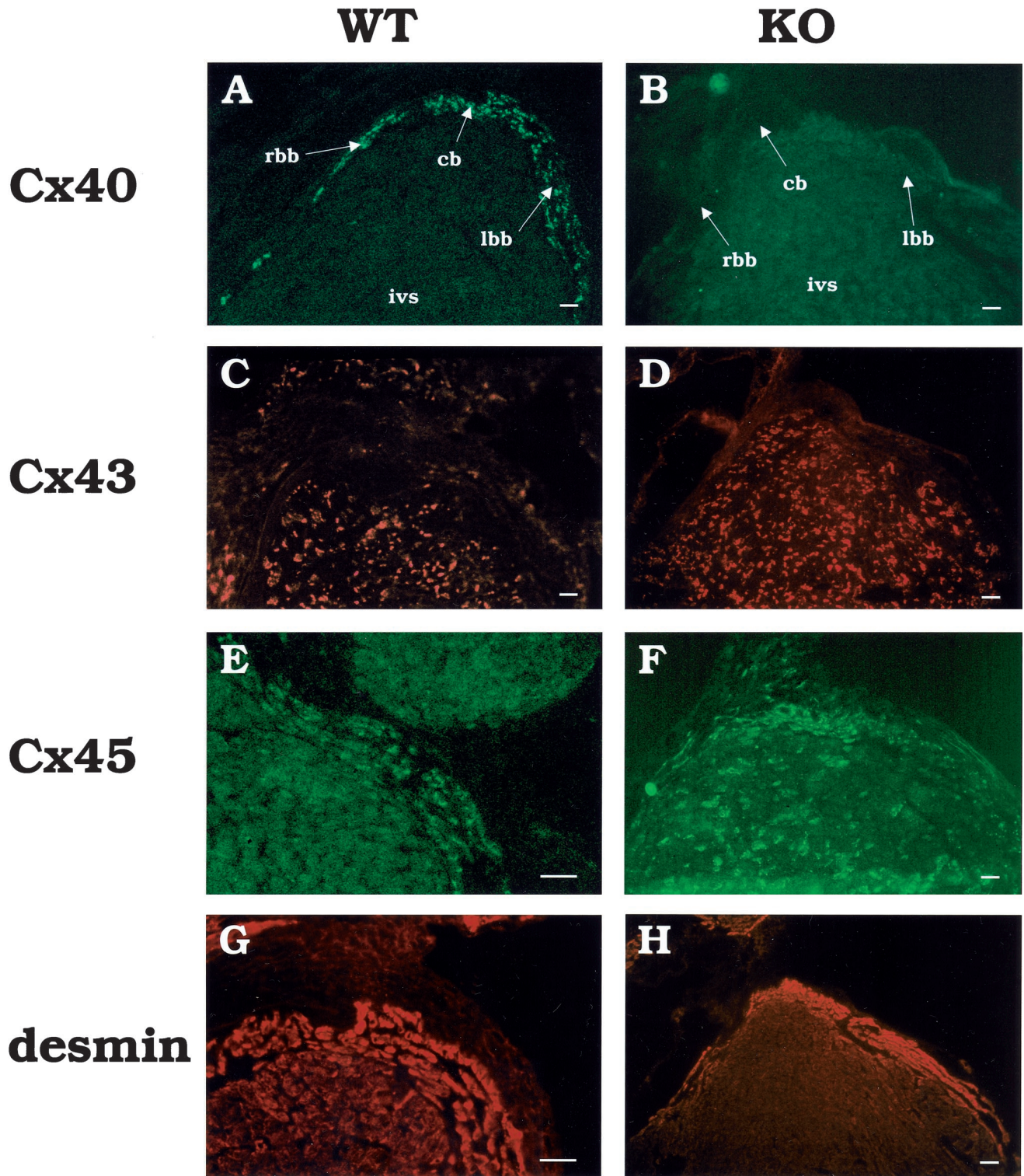


Figure 5. Immunohistochemical analysis of frontal serial sections of wild-type (WT, left) and Cx40 knockout (KO, right) hearts stained for Cx40, Cx43, Cx45, and desmin. Cx40 is located in common bundle and bundle branches and clearly shows difference in size of right (small) and left (wide) bundle branch (A). Cx40 is absent in Cx40 knockout animals (B). Cx43 is located in working myocardium only of both wild-type and Cx40 knockout (C and D). Cx45 is located in His bundle, common bundle (cb), and proximal bundle branches (E and F). Desmin labeling showed clear demarcation of conduction system (G and H). rbb indicates right bundle branch; lbb, left bundle branch; and ivs, interventricular septum. Scale bar=20 μ m.

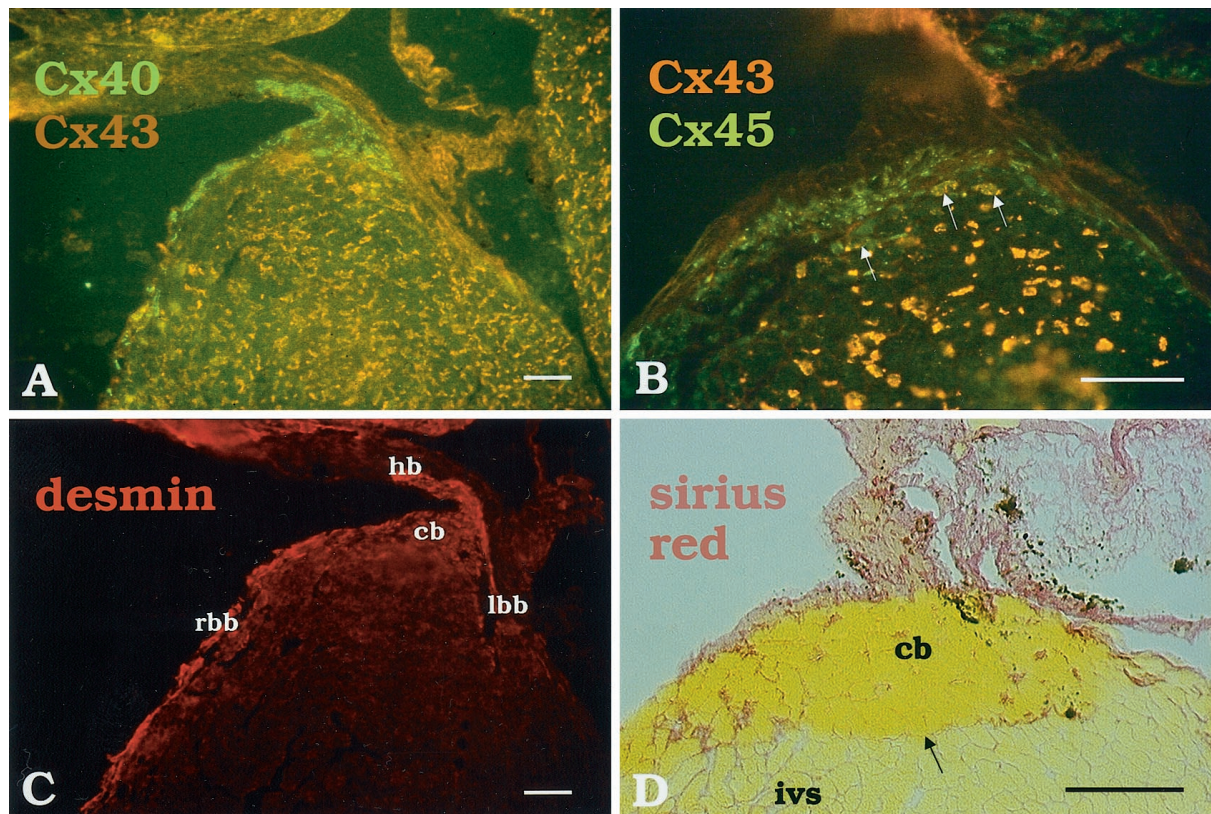


Figure 6. Histochemical analysis of transition zone between common bundle and basal septum. A, Wild-type animal, showing expression of Cx40 and Cx43. In septum and conduction system, these expression patterns are mutually exclusive. B, Double labeling of Cx43 and Cx45 in Cx40 knockout animals showing coexpression of Cx43 and Cx45 at interface between common bundle and septum (marked by arrows). C, Sister section of A stained for desmin showing conduction system. D, Sirius red staining showing fibrotic tissue. Arrow marks strands of myocytes connecting common bundle and interventricular septum. Scale bar=50 μm . hb indicates His bundle; cb, common bundle; lbb, left bundle branch; rbb, right bundle branch; and ivs, interventricular septum.

septum (arrows). In both wild-type and Cx40-deficient animals, electrical continuity is likely from the common bundle to the septum and is mediated by Cx45.

Connective Tissue in the Septum

Figure 6D shows a consecutive section of Figure 6B stained for connective tissue (red). Thin septa of connective tissue are present between the bundle branches and the septum, but connective tissue is virtually absent at the common bundle–septum interface (arrow). There is a clear continuity of myocytes from the common bundle into the septum. Such continuity was found in both wild-type and knockout mice and correlates with basoapical activation of the ventricular septum (Figure 3).

Discussion

RBB But Not LBB in Cx40-Deficient Mice

The electrophysiological data showed RBB block in Cx40-deficient hearts. The immunohistochemical data show that no differences in morphology or Cx expression other than Cx40 are found, excluding any developmental changes. Therefore, our data are highly suggestive for functional block in the RBB of Cx40-deficient mice. The absence of Cx40 also significantly decreases conduction velocity in the LBB from 0.42 to 0.28 $\text{m} \cdot \text{s}^{-1}$. Presumably, conduction along the LBB occurs exclusively by gap junctions formed of Cx45. The

reduced conduction velocity in the LBB is in accordance with observations in model studies and experiments on linear strands of cardiomyocytes. In these systems, a decrease of gap junction coupling results in reduction of conduction velocity.^{20–22} In these model studies, a reduction of conduction velocity from 0.43 to 0.28 $\text{m} \cdot \text{s}^{-1}$ (66% reduction) resulted from a reduction in coupling of ≈ 1.1 to 0.5 μs ($\sim 65\%$).^{20,22}

The absence of Cx40 in the RBB results in conduction block. However, Cx45 labeling is similar in the LBB and RBB, suggesting a similar degree of intercellular coupling. We can only speculate about the reason why RBB block occurs while the left bundle is still conducting, albeit with reduced conduction velocity. Reduced coupling between myocytes alone is not sufficient to explain this discrepancy. Simulations of impulse propagation in strands of myocytes have shown that the electrical coupling between cells must be reduced by at least a factor of 100 to result in conduction block.^{20,22} On the other hand, clinical studies have shown that the vulnerability of the right bundle for conduction block is greater than that of the left bundle.^{23–25} The smaller diameter of the right bundle may play a role because minor discontinuities are more prominent in such bundles for generating activation block by load mismatch.^{26,27} RBB block was also reported as a result of longitudinal dissociation in the His bundle.²⁸ This RBB block could be normalized by pacing of

the His bundle. It is, however, unlikely that longitudinal dissociation was present in our experiments. No conduction abnormalities of fractionated potentials were found in the His bundle activation measurements. Second, the RBB block was located 0.3 to 0.6 mm distal from the AV groove, and finally, the conduction curves measured at the site of the common bundle in Cx40 knockout hearts were not different from control. If a longitudinal dissociation were present in the His bundle, premature stimulation of the atria would have uncovered a progressive AH delay.

Conduction velocity in the His bundle was not different between wild-type and Cx40 knockout. The absence of Cx40, leaving Cx45 as the only Cx in the His bundle, presumably does not reduce intercellular conductance to a level at which conduction velocity is also reduced (also see Reference 22).

The measured RBB block and reduced conduction velocity in the LBB fit well in the previously reported phenotype of the Cx40-deficient mice. One overall finding is that the delay between atrial and ventricular activation (PR interval) is increased,^{13–16} probably caused by the decreased conduction velocity in the working atrial myocardium¹³ and in the conduction system (this study).

Second, an increased QRS duration has been reported in Cx40 knockout mice.^{13–16} Impaired ventricular activation can be due to slow conduction along the ventricle, which is unlikely because Cx40 is normally not expressed in the ventricle or results from abnormal ventricular activation by the conduction system. Impairment of the conduction system in Cx40 knockout mice was suggested by Simon et al,¹⁶ based on the long and split QRS complexes and frontal axis deviation in Cx40-deficient mice. We previously reported that the QRS duration in Cx40-deficient mice was only prolonged in sinus rhythm but not during ventricular pacing, indicating that activation of the ventricles rather than ventricular conduction itself is impaired.¹³ Our experimental results confirm these hypotheses by direct demonstration of RBB activation block in Cx40-deficient mice.

Septal Activation in Wild-Type and Cx40-Deficient Mice

In larger mammals, intraventricular septal activation occurs from left to right and from apex to base.^{29,30} The proximal conduction system is electrically insulated from the septal myocardium by a fibrotic sheet, to ensure ventricular activation after dispersal of the impulse through the conduction system.³¹ Our experiments show that ventricular activation does not follow this pathway in mouse hearts, either wild-type or Cx40-deficient.

Septal measurements of both wild-type and Cx40-deficient hearts always showed a basoapical activation sequence, suggesting a direct electrical connection between the common bundle and the septum. This direct electrical connection indeed seems present, because the fibrotic sheet between the septum and conduction system shows large fenestrations, as reported by Lev and Thamer.³² Furthermore, coexpression of Cx45 and Cx43 was found in the transitional region.

A previous study by Coppen et al¹² reported that in the proximal conduction system, Cx45 is not only coexpressed with Cx40 but that this expression extends through several

cell layers in septal and lateral directions. Coexpression of Cx45 with Cx43 in this region was, however, not reported.

Conclusions

Our study shows that in mice, a continuity exists between the common bundle and the septum, both histological and electrical, and that absence of Cx40 results in RBB block and impaired LBB conduction.

Our observation of an electrical continuity between the common bundle and the septum prohibits comparison of global activation patterns in the mouse and human heart. Our results show, however, that the vulnerability of the RBB is greater than that of the LBB, which is in line with data in patients.^{23–25} This might also be the case for the preferred site of block, which is at a basal site in the RBB rather than at the muscle-Purkinje junction.

Acknowledgments

This study was supported by the Netherlands Heart Foundation (grant 97.184) and the Netherlands Organization for Scientific Research (grant 902-16-193). Work in the Bonn laboratory was supported by the German Research Organization (SFB, grant number 284 [C1]) and the Foundation for Chemical Industry (Dr Willecke). The laboratories of Dr Jongsma and Dr Willecke acknowledge support by the European Community (Biomed QLG1-CT-1999-00516).

References

1. Verheule S, Van Kempen MJA, Te Welscher PHJA, et al. Characterization of gap junction channels in adult rabbit atrial and ventricular myocardium. *Circ Res*. 1997;80:673–681.
2. Bastide B, Neynes L, Ganten D, et al. Gap junction protein connexin40 is preferentially expressed in vascular endothelium and conductive bundles of rat myocardium and is increased under hypertensive conditions. *Circ Res*. 1993;73:1138–1149.
3. Gros D, Jarry-Guichard T, Ten Velde I, et al. Restricted distribution of Connexin40, a gap junctional protein, in mammalian heart. *Circ Res*. 1994;74:839–851.
4. Gourdie RG, Severs NJ, Green CR, et al. The spatial distribution and relative abundance of gap-junctional connexin40 and connexin43 correlate to functional properties of components of the cardiac atrioventricular conduction system. *J Cell Sci*. 1993;105:985–991.
5. Van Kempen MJA, Ten Velde I, Wessels A, et al. Differential connexin expression accommodates cardiac function in different species. *Microsc Res Tech*. 1995;31:420–436.
6. Davis LM, Kanter HL, Beyer EC, et al. Distinct gap junction protein phenotypes in cardiac tissues with disparate conduction properties. *J Am Coll Cardiol*. 1994;24:1124–1132.
7. Davis LM, Rodefeld ME, Green K, et al. Gap junction protein phenotypes of the human heart and conduction system. *J Cardiovasc Electrophysiol*. 1995;6:813–822.
8. Van Kempen MJA, Vermeulen JLM, Moorman AFM, et al. Developmental changes of connexin40 and connexin43 mRNA distribution patterns in the rat heart. *Cardiovasc Res*. 1996;32:886–900.
9. Kanter HL, Saffitz JE, Beyer EC. Cardiac myocytes express multiple gap junction proteins. *Circ Res*. 1992;70:438–444.
10. Darrow BJ, Laing JG, Lampe PD, et al. Expression of multiple connexins in cultured neonatal rat ventricular myocytes. *Circ Res*. 1995;76:381–387.
11. Coppen SR, Dupont E, Rothery S, et al. Connexin45 expression is preferentially associated with the ventricular conduction system in mouse and rat heart. *Circ Res*. 1998;82:232–243.
12. Coppen SR, Severs NJ, Gourdie RG. Connexin45 ($\alpha 6$) expression delineates an extended conduction system in the embryonic and mature rodent heart. *Dev Genet*. 1999;24:82–90.
13. Verheule S, van Batenburg CA, Coenjaerts FE, et al. Cardiac conduction abnormalities in mice lacking the gap junction protein connexin40. *J Cardiovasc Electrophysiol*. 1999;10:1380–1389.

14. Hagendorff A, Schumacher B, Kirchhoff S, et al. Conduction disturbances and increased atrial vulnerability in Connexin40-deficient mice analyzed by transesophageal stimulation. *Circulation*. 1999;99:1508–1515.
15. Kirchhoff S, Nelles E, Hagendorff A, et al. Reduced cardiac conduction velocity and predisposition to arrhythmias in connexin40-deficient mice. *Curr Biol*. 1998;8:299–302.
16. Simon AM, Goodenough DA, Paul DL. Mice lacking connexin40 have cardiac conduction abnormalities characteristic of atrioventricular block and bundle branch block. *Curr Biol*. 1998;8:295–298.
17. Tyrode MV. The mode of action of some purgative salts. *Arch Int Pharmacodyn*. 1910;20:205–223.
18. Van Kempen MJA, Jongsma HJ. Distribution of connexin37, connexin40 and connexin43 in the aorta and coronary artery of several mammals. *Histochem Cell Biol*. 1999;112:479–486.
19. Sweat F, Puchter H, Rosenthal SI. Sirius Red F3Ba as a stain for connective tissue. *Arch Pathol*. 1964;69–72.
20. Shaw RM, Rudy Y. Ionic mechanisms of propagation in cardiac tissue: roles of the sodium and L-type calcium currents during reduced excitability and decreased gap junction coupling. *Circ Res*. 1997;81:727–741.
21. Rohr S, Kucera JP, Kléber AG. Slow conduction in cardiac tissue, I: effects of a reduction of excitability versus a reduction of electrical coupling on microconduction. *Circ Res*. 1998;83:781–794.
22. Jongsma HJ, Wilders R. Gap junctions in cardiovascular disease. *Circ Res*. 2000;86:1193–1197.
23. Golshayan D, Seydoux C, Berguer DG, et al. Incidence and prognostic value of electrocardiographic abnormalities after heart transplantation. *Clin Cardiol*. 1998;21:680–684.
24. Tuzcu EM, Emre A, Goormastic M, et al. Incidence and prognostic significance of intraventricular conduction abnormalities after coronary bypass surgery. *J Am Coll Cardiol*. 1990;16:607–610.
25. Newby KH, Pisano E, Krucoff MW, et al. Incidence and clinical relevance of the occurrence of bundle-branch block in patients treated with thrombolytic therapy. *Circulation*. 1996;94:2424–2428.
26. Rohr S, Kucera JP. Involvement of the calcium inward current in cardiac impulse propagation: induction of unidirectional conduction block by nifedipine and reversal by Bay K 8644. *Biophys J*. 1997;72:754–766.
27. Rohr S, Kucera JP, Fast VG, et al. Paradoxical improvement of impulse conduction in cardiac tissue by partial cellular uncoupling. *Science*. 1997;27:841–844.
28. El-Sherif N, Amay YLF, Schonfield C, et al. Normalization of bundle branch block patterns by distal His bundle pacing: clinical and experimental evidence of longitudinal dissociation in the pathologic his bundle. *Circulation*. 1978;57:473–483.
29. Burchell HB, Essex HE, Pruitt RD. Studies on the spread of excitation through the ventricular myocardium, II: the ventricular septum. *Circulation*. 1952;6:161–171.
30. Durrer D, van Dam RT, Freud GE, et al. Total excitation of the isolated human heart. *Circulation*. 1970;41:899–912.
31. Anderson RH, Becker BE, Trantum-Jensen J, et al. Anatomico-electrophysiological correlations in the conduction system—a review. *Br Heart J*. 1981;45:67–82.
32. Lev M, Thaemert JC. The conduction system of the mouse heart. *Acta Anat*. 1973;85:342–352.